Polynomial Preserving Recovery for Meshes from Delaunay Triangulation or with High Aspect Ratio

Zhimin Zhang
College of Mathematics and Computer Science, Hunan Normal University, Changsha, Hunan 410081, China

Department of Mathematics, Wayne State University, Detroit, MI 48202

Received 1 July 2006; accepted 15 July 2007
Published online 14 December 2007 in Wiley InterScience (www.interscience.wiley.com).
DOI 10.1002/num.20300

A newly developed polynomial preserving gradient recovery technique is further studied. The results are twofold. First, error bounds for the recovered gradient are established on the Delaunay type mesh when the major part of the triangulation is made of near parallelogram triangle pairs with ϵ-perturbation. It is found that the recovered gradient improves the leading term of the error by a factor ϵ. Secondly, the analysis is performed for a highly anisotropic mesh where the aspect ratio of element sides is unbounded. When the mesh is adapted to the solution that has significant changes in one direction but very little, if any, in another direction, the recovered gradient can be superconvergent. Numer Methods Partial Differential Eq 24: 960–971, 2008

Keywords: superconvergence; finite element; adaptive; recovery; Delaunay triangulation; anisotropic mesh

I. INTRODUCTION

Mesh adaptation relies on a posteriori error estimators. While a residual type error estimator depends on the particular form of the underlying differential equations, a recovery type error estimator, such as the Zienkiewicz-Zhu estimator [1–3], employs only numerical solutions. The idea is to construct, from the discrete solution u_h, a recovered gradient $G_h u_h$, which is a “better” approximation for ∇u than ∇u_h (for nonconforming finite element methods, the broken gradient $\nabla_h u_h$ may be applied). By “better” approximation, we mean that $\nabla u - G_h u_h$ is significantly smaller than $\nabla(u - u_h)$ for some norm. Consequently, a computable quantity $G_h u_h - \nabla u_h$ would provide a “good” estimate for the non-computable error $\nabla(u - u_h)$, which can be seen from the following identity

$$\nabla(u - u_h) = \nabla u - G_h u_h + G_h u_h - \nabla u_h. \tag{1.1}$$

Correspondence to: Zhimin Zhang, Department of Mathematics, Wayne State University, Detroit, MI 48202 (e-mail: ag7761@wayne.edu)
Contract grant sponsor: US National Science Foundation; contract grant numbers: DMS-0031807; DMS-0062908

In this article, we will discuss such a gradient recovery method, called Polynomial Preserving Recovery (PPR), under Delaunay type meshes and highly anisotropic meshes.

PPR was first introduced in [4] where the superconvergence of the recovery operator was proved for translation invariant meshes. The uniform boundedness of the recovery operator was established in [5] under a mild mesh condition. PPR for quadrilateral meshes was discussed in [6] and a survey paper [7] briefly summarized the previous results.

To reduce the mesh restriction, a notion of α-condition was discussed in [6, 8]. For a triangular mesh, the α-condition means that any pair of triangles form a near parallelogram with an order $O(h^{1+\alpha})$ distortion for some $\alpha \in [0, 1]$. As for a quadrilateral mesh, the α-condition requires that the distance between the mid-points of two diagonals is of order $O(h^{1+\alpha})$. Under the α-condition, gradient superconvergence of order $O(h^{1+\alpha})$ was established for linear and bilinear finite elements [6, 8].

The α-condition is clearly a more relaxed condition than the "strongly regular" mesh, which requires that the distortion is of order $O(h^2)$ from a parallelogram. Along this line, the reader is referred to [9] for some further discussions on quadrilateral meshes. Indeed, as early as 1984, Shi [10] introduced *Condition B* for quadrilateral meshes which requires that the distortion is of order $o(h)$. Later, Lakhany-Marek-Whiteman [11] studied superconvergence results on $O(h^{1+\alpha})$ type mildly structured triangulations in 2000.

All these mesh conditions are in the asymptotic sense. In other words, these conditions can only be realized when the mesh is refined and a sequence of meshes is constructed. Naturally, the α-condition faces two critics. One is from the mathematical point of view: whether there exists a mesh that satisfies the condition. Another is from the engineering community which argues that in many real life computations, meshes are generated only once or twice, and we seldom actually get into situations when those asymptotic mesh conditions are satisfied. The question is how to access the error in a posteriori sense at one mesh level.

Existence of the mesh that satisfies the α-condition is relatively easier to solve. To access error a posteriorily at one mesh level is not a trivial task. Towards this end, we borrow the domain variation concept from the partial differential equation theory. The assumption is that each element patch with six triangles is an ϵ-deviation of the reference element patch that contains six equilateral triangles (Fig. 1). This "domain variation" can be expressed by a local piecewise linear mapping (2.3), such that a rigorous analysis can be made to access the error created by this ϵ-perturbation. Similar to the analysis of the α-σ domain in [8], we assume that the "most" part of the partition $\mathcal{T}_h$ is made up by such kind of "good" patches, and only "small" portions of $\mathcal{T}_h$ contain "bad" elements. All these will be stated precisely in Section II. Indeed, many meshes generated by an automatic mesh generator fit the aforementioned situation. The most popular case is a mesh generated by the Delaunay triangulation. In this situation, our analysis shows that while the optimal leading error for the gradient approximation is of order $O(h)$, the leading error of the recovered gradient is diminished by the factor ϵ. Therefore, the second term on the right-hand side of (1.1) is the dominant part of the error. In many practical situations, ϵ can be a magnitude.

The main difference of this ϵ-perturbation and the α-condition is that the former accesses the error at one mesh level while the latter needs a sequence of meshes so that the asymptotic condition can be realized. This is the first contribution of the current article. Furthermore, the domain variation technique from the partial differential equation theory is new in finite element analysis.

An important exception is the anisotropic mesh, where the ratio of side lengths of an element is unbounded. In many practical situations, we encounter such meshes, e.g., when the solution of the underlying partial differential equation exhibits boundary layers or internal layers. Our analysis for the two-dimensional setting shows that when the mesh is adapted to the solution which has

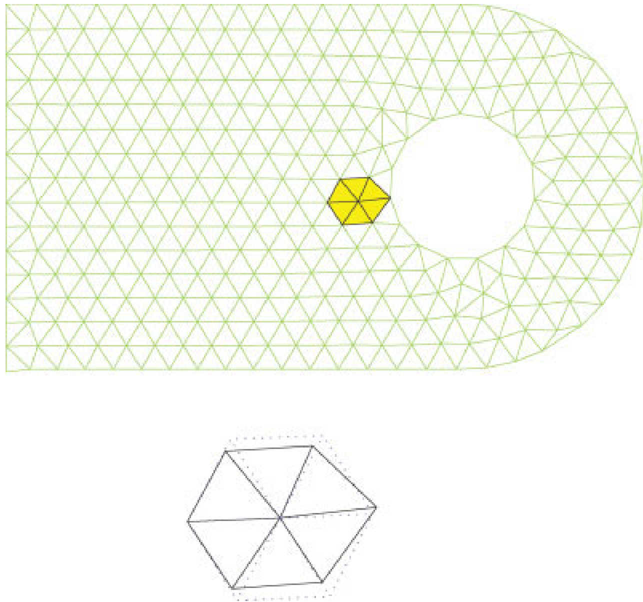

FIG. 1. Example mesh generated by DistMesh 1. [Color figure can be viewed in the online issue, which is available at www.interscience.wiley.com.]

significant changes along one direction and very little variation, if any, along another direction, then the recovered gradient under some uniform anisotropic meshes converges at a rate $O(h^2)$ for the linear element, when compared with the optimal rate $O(h)$. This is the second contribution of the current work. In our analysis, we considered the worst case, where the maximum angle condition [12] can be violated.

As for references regarding a posteriori error estimates and superconvergence related to this article, the reader is referred to [1–3, 12–26].

II. ERROR ESTIMATES UNDER DELAUNAY TRIANGULATION

A. Model Problem

On a polygonal domain $\Omega \subset R^n$, we consider the boundary value problem: To find $u \in H^1(\Omega)$ that satisfies some well posed boundary conditions and

$$B(u, v) = f(v), \quad \forall v \in H^1(\Omega),$$

with the bilinear form defined by

$$\begin{aligned} B(u, v) &= \sum_{i,j=1}^{n} \int_\Omega a_{ij}(x) \frac{\partial u}{\partial x_i} \frac{\partial v}{\partial x_j} dx + \sum_{i=1}^{n} \int_\Omega b_i(x) u \frac{\partial v}{\partial x_i} dx + \int_\Omega cuv dx \\ &= \int_\Omega \nabla u \cdot A(x) \nabla v dx + (u, \boldsymbol{b} \cdot \nabla v) + (cu, v). \end{aligned}$$

We assume the usual strong elliptic condition on $A = A(x)$ and sufficient regularity on all input data, which will be specified later when needed.

We denote $\mathcal{T}_h$, the mesh generated by the Delaunay triangulation and define S_h, the linear C^0 finite element space. Then the finite element approximation $u_h \in S_h$ satisfies

$$B(u_h, v) = f(v), \quad \forall v \in S_h.$$

B. Simplification

Let A_0 be a piecewise constant function such that on each element $\tau \in \mathcal{T}_h$

$$A_0|_\tau = \frac{1}{|\tau|}\int_\tau A(x)dx.$$

Now we define

$$a(u,v) = \int_\Omega \nabla u \cdot A(x)\nabla v dx, \quad a^\tau(u,v) = \int_\tau \nabla u \cdot A_0 \nabla v dx, \quad e_h = u - u_h.$$

Assume that $a_{ij} \in C^{0,\alpha}(\Omega)$, it is straightforward to show that

$$\left| a(e_h, v) - \sum_\tau a^\tau(e_h, v) \right| \le Ch^\alpha |e_h|_{1,\Omega}|v|_{1,\Omega}, \quad \alpha > 0. \tag{2.1}$$

Therefore, we may shift our analysis to $a^\tau(e_h, v)$. Since $A(x)$ is symmetric positive definite, so is $A_0|_\tau$. Then there exists an orthogonal matrix Q_τ such that $A_0|_\tau = Q_\tau^T D_\tau Q_\tau$ with $D_\tau = \text{diag}(d_1^\tau, \ldots, d_n^\tau)$. By changing of variable $x = Q_\tau z$, we have

$$a^\tau(e_h, v) = \int_{\tau_z} \nabla_z e_h \cdot D_\tau \nabla_z v \det Q_\tau dz. \tag{2.2}$$

Note that $\nabla_z = Q_\tau \nabla_x$, $\det Q_\tau = \pm 1$, and τ_z is obtained by rotating τ. Therefore, without loss of generality we may concentrate on the second order form

$$\int_\tau \nabla e_h \cdot D_\tau \nabla v dx = \int_\tau \sum_{i=1}^n d_i^\tau \frac{\partial e_h}{\partial x_i}\frac{\partial v}{\partial x_i} dx, \quad d_i^\tau > 0,$$

and estimate the bilinear form

$$B(e_h, v) = \sum_{\tau \in \mathcal{T}_h} \int_\tau \nabla e_h \cdot D_\tau \nabla v dx + \int_\Omega e_h(\boldsymbol{b} \cdot \nabla v + cv)dx.$$

Remark. It is not necessary to carry on the similar simplification for piecewise constants $\boldsymbol{b}$ and c, since they involve in higher-order error terms in analysis.

C. Domain Variation

Now we concentrate on the two-dimensional case. We assume that $\mathcal{T}_h$ can be separated into two parts

$$\mathcal{T}_h = \mathcal{T}_{0,h} \cup \mathcal{T}_{1,h}, \quad \bigcup_{\tau \in \mathcal{T}_{i,h}} \bar{\tau} = \bar{\Omega}_{i,h}, \quad \bar{\Omega} = \bar{\Omega}_{0,h} \cup \bar{\Omega}_{1,h},$$

such that:

1. Any two triangles that share a common edge in $\mathcal{T}_{0,h}$ form a convex quadrilateral which is an ϵ-perturbation from a parallelogram.
2. $\Omega_{1,h}$ has a small measure: $|\Omega_{1,h}| = O(h^\sigma)$ $(\sigma > 0)$.

This assumption is called ϵ-σ mesh condition. Note that a mesh generated by the Delaunay triangulation satisfies this mesh condition. An example is illustrated by Fig. 1, which is produced by a public domain mesh generator "DistMesh". We see that except at most one layer boundary elements, which has a small measure $O(h)(\sigma = 1)$, the majority of patches are formed by six near equilateral triangles.

Remark. There is an essential difference of the α-σ mesh discussed in [6, 8] and this ϵ-σ mesh. We are able to access the error in only one mesh with the latter, while a sequence of meshes are needed to realize the former.

To analyze the finite element approximation error under the ϵ-σ mesh, we adopt the notion of domain variation from the partial differential equation theory [27]:

$$y = x + \epsilon\eta(x), \tag{2.3}$$

where η is a piecewise linear function (therefore, $\frac{\partial \eta_i}{\partial x_j}$ is a constant in each element) and $\nabla_x \eta$ is bounded uniformly in ϵ and h. The piecewise linear mapping η is constructed in such a way that in the y-coordinates, the image of $\mathcal{T}_{0,h}$ contains only parallelogram triangle pairs. Simple calculation shows that

$$\frac{\partial x_i}{\partial y_j} = \delta_{ij} - \epsilon\frac{\partial \eta_i}{\partial x_j} + O(\epsilon^2), \quad \frac{\partial y_i}{\partial x_j} = \delta_{ij} + \epsilon\frac{\partial \eta_i}{\partial x_j};$$

$$\det\left(\frac{\partial y_i}{\partial x_j}\right) = 1 + \epsilon \mathrm{div}_x \eta + O(\epsilon^2), \quad \det\left(\frac{\partial x_i}{\partial y_j}\right) = 1 - \epsilon \mathrm{div}_x \eta + O(\epsilon^2);$$

$$\frac{\partial u}{\partial y_j} = \sum_{i=1}^{n} \frac{\partial u}{\partial x_i}\frac{\partial x_i}{\partial y_j} = \frac{\partial u}{\partial x_j} - \epsilon\sum_{i=1}^{n} \frac{\partial u}{\partial x_i}\frac{\partial \eta_i}{\partial x_j} + O(\epsilon^2);$$

$$\frac{\partial u}{\partial x_j} = \sum_{k=1}^{n} \frac{\partial u}{\partial y_k}\frac{\partial y_k}{\partial x_j} = \frac{\partial u}{\partial y_j} + \epsilon\sum_{k=1}^{n} \frac{\partial u}{\partial y_k}\frac{\partial \eta_k}{\partial x_j}. \tag{2.4}$$

$$\frac{\partial^2 u}{\partial x_i \partial x_j} = \frac{\partial}{\partial y_i}\left(\frac{\partial u}{\partial x_j}\right) + \epsilon\sum_{l=1}^{n} \frac{\partial}{\partial y_l}\left(\frac{\partial u}{\partial x_j}\right)\frac{\partial \eta_l}{\partial x_i}$$

$$= \frac{\partial^2 u}{\partial y_i \partial y_j} + \epsilon\sum_{k=1}^{n} \frac{\partial^2 u}{\partial y_k \partial y_i}\frac{\partial \eta_k}{\partial x_j} + \epsilon\sum_{k=1}^{n} \frac{\partial^2 u}{\partial y_k \partial y_j}\frac{\partial \eta_k}{\partial x_i} + \epsilon^2\sum_{k,l=1}^{n} \frac{\partial^2 u}{\partial y_k \partial y_l}\frac{\partial \eta_k}{\partial x_j}\frac{\partial \eta_l}{\partial x_i}. \tag{2.5}$$

Higher order partial derivatives can be obtained in a similar manner.

Here we keep in mind that $n = 2$ although (2.4) and (2.5) are valid for any dimensional setting.

D. Error Estimates

Let $e_I = u - u_I$ where $u_I \in S_h$ is the Lagrange linear interpolation of u. By direct calculation, we have

$$
\begin{aligned}
\int_\tau \nabla e_I \cdot D_\tau \nabla v dx &= \sum_{i=1}^{n} \int_\tau d_i^\tau \frac{\partial e_I}{\partial x_i} \frac{\partial v}{\partial x_i} dx \\
&= \sum_{i=1}^{n} \int_{\tau_y} d_i^\tau \left(\frac{\partial e_I}{\partial y_i} + \epsilon \sum_{k=1}^{n} \frac{\partial e_I}{\partial y_k} \frac{\partial \eta_k}{\partial x_i} \right) \left(\frac{\partial v}{\partial y_i} + \epsilon \sum_{l=1}^{n} \frac{\partial v}{\partial y_l} \frac{\partial \eta_l}{\partial x_i} \right) (1 - \epsilon \mathrm{div}_x \eta + O(\epsilon^2)) dy \\
&= I_0(\tau) + \epsilon I_1(\tau) + \epsilon^2 I_2(\tau).
\end{aligned} \tag{2.6}
$$

where

$$
I_0(\tau) = \sum_{i=1}^{n} d_i^\tau \int_{\tau_y} \frac{\partial e_I}{\partial y_i} \frac{\partial v}{\partial y_i} dy = \int_{\tau_y} \nabla_y e_I \cdot D_\tau \nabla_y v dy;
$$

$$
I_1(\tau) = \sum_{i=1}^{n} \int_{\tau_y} d_i^\tau \left(-\frac{\partial e_I}{\partial y_i} \frac{\partial v}{\partial y_i} \mathrm{div}_x \eta + \frac{\partial e_I}{\partial y_i} \sum_{l=1}^{n} \frac{\partial v}{\partial y_l} \frac{\partial \eta_l}{\partial x_i} + \frac{\partial v}{\partial y_i} \sum_{k=1}^{n} \frac{\partial e_I}{\partial y_k} \frac{\partial \eta_k}{\partial x_i} \right) dy;
$$

and the rest is I_2. Because of the assumption that $\nabla_x \eta$ is uniformly bounded in ϵ and h, we have

$$
|I_2(\tau)| \lesssim |I_1(\tau)|. \tag{2.7}
$$

Furthermore, in the y-coordinate system, the image of $\Omega_{0,h}$ under the triangulation $\mathcal{T}_{0,h}$ is formed by triangles where each pair makes a parallelogram. Under this y-coordinate system, we define a "broken norm" as following

$$
\|u\|_{k,\Omega_y}^2 = \sum_{\tau \in \mathcal{T}_{0,h}} \|u\|_{k,\tau_y}^2.
$$

By the standard finite element super-convergence analysis (see, e.g., [19, 23]), we are able to derive

$$
\left| \sum_{\tau \in \mathcal{T}_{0,h}} I_0(\tau) \right| \lesssim h^{3/2} \|u\|_{3,\Omega_y} |v|_{1,\Omega_y} \lesssim h^{3/2} (\|u\|_{3,\Omega_{0,h}} + O(\epsilon)) |v|_{1,\Omega}, \tag{2.8}
$$

due to cancellations between parallel sides of adjacent triangles. As for the term $I_1(\tau)$, the standard estimate will apply,

$$
\left| \sum_{\tau \in \mathcal{T}_{0,h}} I_1(\tau) \right| \lesssim h \|u\|_{2,\Omega_y} |v|_{1,\Omega_y} \lesssim h (\|u\|_{2,\Omega_{0,h}} + O(\epsilon)) |v|_{1,\Omega}. \tag{2.9}
$$

Combining (2.6)–(2.9), we obtain

$$
\left| \sum_{\tau \in \mathcal{T}_{0,h}} \int_\tau \nabla e_I \cdot D_\tau \nabla v dx \right| \lesssim (h^{3/2} (\|u\|_{3,\Omega_{0,h}} + \epsilon) + h\epsilon (\|u\|_{2,\Omega_{0,h}} + \epsilon)) |v|_{1,\Omega}. \tag{2.10}
$$

Summarize and we have the following interpolation theorem on $\mathcal{T}_{0,h}$.

Theorem 2.1. *Let $u \in H^3(\Omega_{0,h})$ and $u_I \in S_h$ be its Lagrange linear interpolation. Then the error bound (2.10) is valid.*

Polynomial Preserving Gradient Recovery Following [4], we introduce a gradient recovery operator $G_h : S_h \to S_h \times S_h$. For linear element, all we need is to define $G_h u_h$ at each node z_i of the triangulation $\mathcal{T}_h$:

$$G_h u_h(z_i) = \sum_j \vec{C}_{ij} u_h(z_{ij}), \quad \sum_j \vec{C}_{ij} = \vec{0},$$

where $\vec{C}_{ij}$ are coefficients of some finite difference schemes. We refer to [4] for choices of $\vec{C}_{ij}$ in some special situations. We see that the recovered gradient at z_i is a linear combination of some nearby nodal values of the finite element solution. As far as the current paper is concerned, we only need the following two properties:

1. Polynomial preserving: When at least six nodes z_{ij} are not on a conic curve, we have

$$\|\nabla u - G_h u_I\| \lesssim h^2 |u|_{3,\Omega}.$$

2. Boundedness: When there are no two adjacent angles on an element patch adding up to exceed π, we have

$$\|G_h v\| \lesssim |v|_{1,\Omega}, \quad \forall v \in S_h.$$

The reader is referred to [4–6] for details regarding the recovery operator G_h.

Theorem 2.2. *Let $u \in H^3(\Omega) \cap W^2_\infty(\Omega)$ and $u_h \in S_h$ be the solution of the model problem and its linear finite element approximation, respectively. Assume (a) the ϵ-σ mesh condition, (b) the maximum angle condition, and (c) the discrete inf-sup condition. Then the polynomial preserving gradient recovery operator G_h leads to superconvergence in the sense that:*

$$\|\nabla u - G_h u_h\| \lesssim h^2 \|u\|_{3,\Omega} + h^{3/2}(\|u\|_{3,\Omega_{0,h}} + \epsilon) + h\epsilon(\|u\|_{2,\Omega_{0,h}} + \epsilon) + h^{1+\sigma/2}|u|_{2,\infty,\Omega}.$$

Proof. By the triangle inequality and the polynomial preserving property,

$$\|\nabla u - G_h u_h\| \le \|\nabla u - G_h u_I\| + \|G_h(u_I - u_h)\| \lesssim h^2|u|_{3,\Omega} + |u_h - u_I|_{1,\Omega}. \tag{2.11}$$

The analysis for the second term on the right-hand side under conditions (a) and (b) is proceeded as the following:

$$\left| \sum_{\tau \in \mathcal{T}_{1,h}} \int_\tau \nabla e_I \cdot D_\tau \nabla v dx \right| \lesssim h|u|_{2,\infty,\Omega} \sum_{\tau \in \mathcal{T}_{1,h}} \int_\tau |\nabla v| dx \lesssim h^{1+\sigma/2} |u|_{2,\infty,\Omega} \|\nabla v\|_{0,\Omega}, \tag{2.12}$$

and (by the standard approximation theory)

$$\left| \int_\Omega e_I(\boldsymbol{b} \cdot \nabla v + cv) dx \right| \lesssim h^2 |u|_{2,\Omega} |v|_{1,\Omega}. \tag{2.13}$$

Based on (2.10), (2.12), and (2.13), we derive

$$|B(e_I, v)| \lesssim (h^{3/2}(\|u\|_{3,\Omega_{0,h}} + \epsilon) + h\epsilon(\|u\|_{2,\Omega} + \epsilon) + h^{1+\sigma/2}|u|_{2,\infty,\Omega})|v|_{1,\Omega}. \tag{2.14}$$

Using the discrete inf-sup condition and the strong elliptic assumption, we then have

$$\begin{aligned} \|u_I - u_h\|_{1,\Omega} &\lesssim \sup_{v \in S_h} \frac{B(u_h - u_I, v)}{\|v\|_{1,\Omega}} = \sup_{v \in S_h} \frac{B(e_I, v)}{\|v\|_{1,\Omega}} \\ &\lesssim h^{3/2}(\|u\|_{3,\Omega_{0,h}} + \epsilon) + h\epsilon(\|u\|_{2,\Omega} + \epsilon) + h^{1+\sigma/2}|u|_{2,\infty,\Omega}. \end{aligned} \tag{2.15}$$

The conclusion follows by substituting (2.15) into (2.11). ∎

Remark. We see that the recovered gradient $G_h u_h$ is "closer" to the exact gradient ∇u than ∇u_h as long as the majority of triangle pairs deviate not too much from parallelograms.

Remark. The estimates (2.12) and (2.13) require the maximum angle condition [12]. In the next section, we shall demonstrate that when solution has special features in one direction and the mesh is properly adapted to the solution, violation of the maximum angle condition can be legal.

III. ERROR ESTIMATES UNDER ANISOTROPIC MESHES

In this section, we consider an anisotropic mesh with high aspect ratio in 2D, see Fig. 2, where the coefficients of the recovery operator G_h are provided. It is worthy to point out that we consider the worst case where the maximum angle condition is violated at the extremal case $\theta \to 0$. Other compressed (in one direction) triangulations such as the regular, Chevron, and Unit-Jack patterns can be discussed similarly with less restrictive assumptions.

It is straightforward to verify that the recovery operator in figures 2 satisfies

$$G_h v(0,0)^T = \left(\sum_{j=1}^{6} \frac{\partial v}{\partial x}\bigg|_{\tau_j}, \frac{1}{4}\left[\frac{\partial v}{\partial y}\left(\frac{h}{2}, 0+\right) + \frac{\partial v}{\partial y}\left(\frac{h}{2}, 0-\right) + \frac{\partial v}{\partial y}\left(-\frac{h}{2}, 0+\right) + \frac{\partial v}{\partial y}\left(-\frac{h}{2}, 0-\right) \right] \right),$$

for any $v \in S_h$. We see that the recovered x-derivative at the center node is the average of derivatives on all six elements and the recovered y-derivative at the center is the average of derivatives on the four congruent triangles. Therefore, $\|G_h\|$ is uniformly bounded with bounding constant 1 although the maximum angle condition is violated when $\theta \to 0$. Other types of anisotropic meshes can be studied similarly.

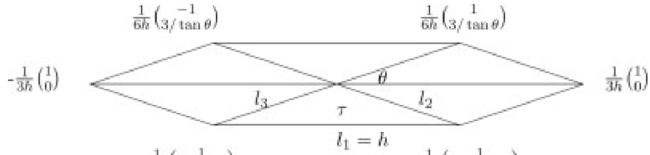

FIG. 2. Anisotropic mesh.

To simplify the matter, we analyze the case $\boldsymbol{b} = 0$ and $c = 0$. We need the following integral identity [17] for $v_h \in P_1(\tau)$,

$$\int_\tau \nabla(u - u_I) \cdot \mathcal{D}_\tau \nabla v_h = \sum_{k=1}^{3} \int_{e_k} \frac{\xi_k q_k}{2\sin\theta_k} \left\{ \left(\ell_{k+1}^2 - \ell_{k-1}^2\right) \frac{\partial^2 u}{\partial \boldsymbol{t}_k^2} + 4|\tau| \frac{\partial^2 u}{\partial \boldsymbol{t}_k \partial \boldsymbol{n}_k} \right\} \frac{\partial v_h}{\partial \boldsymbol{t}_k}$$
$$- \int_\tau \sum_{k=1}^{3} \frac{\ell_k \xi_k}{2\sin^2\theta_k} \left\{ \ell_{k+1}\psi_{k-1} \frac{\partial^3 u}{\partial \boldsymbol{t}_{k+1}^2 \partial \boldsymbol{t}_{k-1}} + \ell_{k-1}\psi_{k+1} \frac{\partial^3 u}{\partial \boldsymbol{t}_{k-1}^2 \partial \boldsymbol{t}_{k+1}} \right\} \frac{\partial v_h}{\partial \boldsymbol{t}_k}, \quad (3.1)$$

where k is modulo 3, angle θ_k is opposite of side l_k (with length ℓ_k), λ_k is the nodal basis function, $q_k = \lambda_{k+1}\lambda_{k-1}$, $\psi_k = \lambda_k(1 - \lambda_k)$, and $\boldsymbol{t}_k$ ($\boldsymbol{n}_k$) is the counter-clockwise unit tangential (outer-normal) vector on side l_k. Finally, $\xi_k = \boldsymbol{n}_{k-1} \cdot \mathcal{D}_\tau \boldsymbol{n}_{k+1}$.

In Fig. 2, we let $\theta_2 = \theta_3 = \theta$. It is straightforward to verify

$$\frac{\partial^3 u}{\partial \boldsymbol{t}_2^2 \partial \boldsymbol{t}_3} = -\frac{\partial^3 u}{\partial x^3}\cos^3\theta + \frac{\partial^3 u}{\partial x^2 \partial y}\cos^2\theta\sin\theta + \frac{\partial^3 u}{\partial x \partial y^2}\cos\theta\sin^2\theta - \frac{\partial^3 u}{\partial y^3}\sin^3\theta.$$

Note that $\sin\theta_1 = \sin(\pi - \theta_2 - \theta_3) = \sin 2\theta$, therefore,

$$\frac{4\cos\theta}{\sin^2\theta_1}\frac{\partial^3 u}{\partial \boldsymbol{t}_2^2 \partial \boldsymbol{t}_3} = -\frac{\partial^3 u}{\partial x^3}\cot^2\theta + \frac{\partial^3 u}{\partial x^2 \partial y}\cot\theta + \frac{\partial^3 u}{\partial x \partial y^2} - \frac{\partial^3 u}{\partial y^3}\tan\theta. \quad (3.2)$$

Similarly,

$$\frac{4\cos\theta}{\sin^2\theta_1}\frac{\partial^3 u}{\partial \boldsymbol{t}_2 \partial \boldsymbol{t}_3^2} = -\frac{\partial^3 u}{\partial x^3}\cot^2\theta - \frac{\partial^3 u}{\partial x^2 \partial y}\cot\theta + \frac{\partial^3 u}{\partial x \partial y^2} + \frac{\partial^3 u}{\partial y^3}\tan\theta; \quad (3.3)$$

$$\frac{\cos\theta}{\sin^2\theta_2}\frac{\partial^3 u}{\partial \boldsymbol{t}_3 \partial \boldsymbol{t}_1^2} = -\frac{\partial^3 u}{\partial x^3}\cot^2\theta + \frac{\partial^3 u}{\partial x^2 \partial y}\cot\theta, \quad (3.4)$$

$$\frac{1}{\sin^2\theta_2}\frac{\partial^3 u}{\partial \boldsymbol{t}_3^2 \partial \boldsymbol{t}_1} = \frac{\partial^3 u}{\partial x^3}\cot^2\theta - 2\frac{\partial^3 u}{\partial x^2 \partial y}\cot\theta + \frac{\partial^3 u}{\partial x \partial y^2}. \quad (3.5)$$

The expressions of

$$\frac{\cos\theta}{\sin^2\theta_3}\frac{\partial^3 u}{\partial \boldsymbol{t}_1^2 \partial \boldsymbol{t}_2}, \quad \frac{1}{\sin^2\theta_3}\frac{\partial^3 u}{\partial \boldsymbol{t}_1 \partial \boldsymbol{t}_2^2}$$

are similar. Furthermore,

$$\xi_1 = d_2^\tau \cos^2\theta - d_1^\tau \sin^2\theta, \quad \xi_2 = \xi_3 = -d_2^\tau \cos\theta. \quad (3.6)$$

Assume uniform mesh of pattern Fig. 2 is applied to a local region $\Omega_a \subset \Omega$. Then for $v \in S_h^0(\Omega_a)$, we have

$$\sum_{\tau \subset \Omega_a} \int_\tau \nabla e_I \cdot \mathcal{D}_\tau \nabla v =$$
$$- \sum_{\tau \subset \Omega_a} \int_\tau \sum_{k=1}^{3} \frac{\ell_k \xi_k}{2\sin^2\theta_k} \left\{ \ell_{k+1}\psi_{k-1} \frac{\partial^3 u}{\partial \boldsymbol{t}_{k+1}^2 \partial \boldsymbol{t}_{k-1}} + \ell_{k-1}\psi_{k+1} \frac{\partial^3 u}{\partial \boldsymbol{t}_{k-1}^2 \partial \boldsymbol{t}_{k+1}} \right\} \frac{\partial v}{\partial \boldsymbol{t}_k}. \quad (3.7)$$

Note that all edge terms are cancelled due to the parallelogram structure.

Let $\ell_1 = h$, then $\ell_2 = \ell_3 = h/(2\cos\theta)$. Applying (3.6), we obtain

$$\frac{\ell_1\xi_1}{2\sin^2\theta_1}\left(\ell_2\psi_3\frac{\partial^3 u}{\partial \boldsymbol{t}_2^2\partial \boldsymbol{t}_3} + \ell_3\psi_2\frac{\partial^3 u}{\partial \boldsymbol{t}_2\partial \boldsymbol{t}_3^2}\right)$$
$$= \frac{h^2}{2}\left(d_2^\tau - d_1^\tau\tan^2\theta\right)\left(\psi_3\frac{\cos\theta}{2\sin^2\theta_1}\frac{\partial^3 u}{\partial \boldsymbol{t}_2^2\partial \boldsymbol{t}_3} + \psi_2\frac{\cos\theta}{2\sin^2\theta_1}\frac{\partial^3 u}{\partial \boldsymbol{t}_2\partial \boldsymbol{t}_3^2}\right); \quad (3.8)$$

$$\frac{\ell_2\xi_2}{2\sin^2\theta_2}\left(\ell_3\psi_1\frac{\partial^3 u}{\partial \boldsymbol{t}_3^2\partial \boldsymbol{t}_1} + \ell_1\psi_3\frac{\partial^3 u}{\partial \boldsymbol{t}_3\partial \boldsymbol{t}_1^2}\right)$$
$$= -\frac{h^2 d_2^\tau}{4}\left(\psi_1\frac{1}{2\sin^2\theta\cos\theta}\frac{\partial^3 u}{\partial \boldsymbol{t}_3^2\partial \boldsymbol{t}_1} + \psi_3\frac{1}{\sin^2\theta}\frac{\partial^3 u}{\partial \boldsymbol{t}_3\partial \boldsymbol{t}_1^2}\right); \quad (3.9)$$

$$\frac{\ell_3\xi_3}{2\sin^2\theta_3}\left(\ell_1\psi_2\frac{\partial^3 u}{\partial \boldsymbol{t}_1^2\partial \boldsymbol{t}_2} + \ell_2\psi_1\frac{\partial^3 u}{\partial \boldsymbol{t}_1\partial \boldsymbol{t}_2^2}\right)$$
$$= -\frac{h^2 d_2^\tau}{4}\left(\psi_2\frac{1}{\sin^2\theta}\frac{\partial^3 u}{\partial \boldsymbol{t}_1^2\partial \boldsymbol{t}_2} + \psi_1\frac{1}{2\sin^2\theta\cos\theta}\frac{\partial^3 u}{\partial \boldsymbol{t}_1\partial \boldsymbol{t}_2^2}\right). \quad (3.10)$$

Substituting (3.8)–(3.10) into (3.7) and applying (3.2)–(3.5), we derive

$$\left|\sum_{\tau\subset\Omega_a}\int_\tau \nabla e_I\cdot\mathcal{D}_\tau\nabla v\right|$$
$$\lesssim h^2\left(\left\|\frac{\partial^3 u}{\partial x^3}\right\|_{0,\Omega_a}\left(d_2^\tau\cot^2\theta + d_1^\tau\right) + \left\|\frac{\partial^3 u}{\partial x^2\partial y}\right\|_{0,\Omega_a}\left(d_2^\tau\cot\theta + d_1^\tau\tan\theta\right)\right.$$
$$\left. + \left\|\frac{\partial^3 u}{\partial x\partial y^2}\right\|_{0,\Omega_a}\left(d_2^\tau + d_1^\tau\tan^2\theta\right) + \left\|\frac{\partial^3 u}{\partial y^3}\right\|_{0,\Omega_a}\left(d_2 + d_1^\tau\tan^2\theta\right)\tan\theta\right)|v|_{1,\Omega_a}. \quad (3.11)$$

The above argument can be summarized into the following theorem.

Theorem 3.1. *Let $u\in H^3(\Omega_a)$, $\Omega_a\subset\Omega$ contains anisotropic uniform triangles of type in Fig. 2 with $\theta\in(0,\pi/4]$ ($\theta\in(\pi/4,\pi/2)$ can be treated similarly by shifting the focus directions). Assume that*

$$d_2^\tau\left(\left\|\frac{\partial^3 u}{\partial x^3}\right\|_{0,\Omega_a}\cot^2\theta + \left\|\frac{\partial^3 u}{\partial x^2\partial y}\right\|_{0,\Omega_a}\cot\theta\right)\le K \quad (3.12)$$

with a constant K independent of θ. Here d_2^τ is the diagonal entry of D_τ defined in (2.2). Then we have

$$\left|\sum_{\tau\subset\Omega_a}\int_\tau \nabla e_I\cdot\mathcal{D}_\tau\nabla v_h\right|\lesssim h^2|v_h|_{1,\Omega_a},\quad \forall v_h\in S_h^0(\Omega_a).$$

Remark. From Theorem 3.1, we see that when u has very little activity in the x-direction, the degenerating limit $\theta=0$ in a sample triangle τ can be allowed, which is equivalent to allow the maximum angle in τ be as close as possible to π. The rate of convergence is maintained at $O(h^2)$.

The practical cases for the assumption in Theorem 3.1 are singularly perturbed problems, which exhibit boundary or internal layers. In a layer region, the solution moves rapidly in one direction while changes very little in other directions. When the mesh is adapted to the solution, even the maximum angle condition can be violated and the numerical approximation still maintains the optimal even superconvergence rate. Indeed this behavior was observed in practical computation [20].

By the similar argument as in Theorem 2.2, we have the following theorem.

Theorem 3.2. *Let $u \in H^3(\Omega) \cap W^2_\infty(\Omega)$ and $u_h \in S_h$ be the solution of the model problem and its linear finite element approximation, respectively. Assume (a) ϵ-σ mesh condition, (b) $\Omega_a \subset \Omega_{0,h}$ contains anisotropic uniform triangles of type in Fig. 2 with $\theta \in (0, \pi/4]$ and elements in $\Omega \backslash \Omega_a$ satisfy the maximum angle condition, and (c) the discrete inf-sup condition. Furthermore, assume that (3.12) is valid with the constant K independent of θ. Then the polynomial preserving gradient recovery operator G_h has the following error bound:*

$$\|\nabla u - G_h u_h\| \lesssim h^2 \|u\|_{3,\Omega} + h^{3/2}(\|u\|_{3,\Omega_{0,h}} + \epsilon) + h\epsilon(\|u\|_{2,\Omega} + \epsilon) + h^{1+\sigma/2}|u|_{2,\infty,\Omega}.$$

In conclusion, when a part of Ω is decomposed by the Delaunay triangulation, another part has uniform anisotropic elements with high aspect ratio, which adapted to the solution behavior, the polynomial preserving recovery still results in much improved gradient. This recovered gradient will in turn provide a reliable a posteriori error estimator in the sense that

$$\frac{\|\nabla(u - u_h)\|}{\|G_h u_h - \nabla u_h\|} \approx 1.$$

As a final remark, our error estimates can be "localized" by applying the interior analysis technique, following the same line of argument as for the α-σ mesh condition in [8].

References

1. O. C. Zienkiewicz and J. Z. Zhu, A simple error estimator and adaptive procedure for practical engineering analysis, Int J Numer Methods Eng 24 (1987), 337–357.
2. O. C. Zienkiewicz and J. Z. Zhu, The superconvergence patch recovery and a posteriori error estimates. I. The recovery technique, Int J Numer Methods Eng 33 (1992), 1331–1364.
3. O. C. Zienkiewicz and J. Z. Zhu, The superconvergence patch recovery and a posteriori error estimates. II. Error estimates and adaptivity, Int J Numer Methods Eng 33 (1992), 1365–1382.
4. Z. Zhang and A. Naga, A new finite element gradient recovery method: superconvergence property, SIAM J Sci Comput 26 (2005), 1192–1213.
5. A. Naga and Z. Zhang, A posteriori error estimates based on polynomial preserving recovery, SIAM J Numer Anal 42 (2004), 1780–1800.
6. Z. Zhang, Polynomial preserving gradient recovery and a posteriori estimate for bilinear element on irregular quadrilaterals, Int J Numer Anal Model 1 (2004), 1–24.
7. Z. Zhang, Polynomial preserving recovery for anisotropic and irregular grids, J Comput Math 22 (2004), 331–340.
8. J. Xu and Z. Zhang, Analysis of recovery type a posteriori error estimators for mildly structured grids, Math Comput 73 (2004), 1139–1152.
9. P. B. Ming and Z.-C. Shi, Quadrilateral mesh revisited, Comput Methods Appl Mech Eng 191 (2002), 5671–5682.

10. Z.-C. Shi, A convergence condition for the quadrilateral Wilson element, Numer Math 44 (1984), 349–361.

11. A. M. Lakhany, I. Marek, and J. R. Whiteman, Superconvergence results on mildly structured triangulations, Comput Methods Appl Mech Eng 189 (2000), 1–75.

12. I. Babuška and A. K. Aziz, On the angle condition in the finite element method, SIAM J Numer Anal 13 (1976), 214–226.

13. M. Ainsworth and J. T. Oden, A posteriori error estimation in finite element analysis, Wiley Interscience, New York, 2000.

14. I. Babuška and W. C. Rheinboldt, A posteriori error estimates for the finite element method, Int J Numer Methods Eng 12 (1978), 1597–1615.

15. I. Babuška and T. Strouboulis, The finite element method and its reliability, Oxford University Press, London, 2001.

16. R. E. Bank and A. Weiser, Some a posteriori error estimators for elliptic partial differential equations, Math Comput 44 (1985), 283–301.

17. R. E. Bank and J. Xu, Asymptotically exact a posteriori error estimators. I: Grid with superconvergence, SIAM J Numer Anal 41 (2003), 2294–2312.

18. C. Carstensen and S. Bartels, Each averaging technique yields reliable a posteriori error control in FEM on unstructured grids. I. Low order conforming, nonconforming, and mixed FEM, Math Comput 71 (2002), 945–969.

19. C. M. Chen and Y. Q. Huang, High accuracy theory of finite element methods, Hunan Science Press, Hunan, China, 1995, (in Chinese).

20. J. Dompierre, M.-G. Vallet, Y. Bourgault, M. Fortin, and W. G. Habashi, Anisotropic mesh adaptation: towards user-independent, mesh-independent and solver-independent CFD. III. Unstructured meshes, Int J Numer Methods Fluids 39 (2002), 675–702.

21. W. Hoffmann, A. H. Schatz, L. B. Wahlbin, and G. Wittum, Asymptotically exact a posteriori estimators for the pointwise gradient error on each element in irregular meshes. I. A smooth problem and globally quasi-uniform meshes, Math Comput 70 (2001), 897–909.

22. M. Křížek, P. Neittaanmäki, and R. Stenberg, editors, Finite element methods: superconvergence, post-processing, and a posteriori estimates, Lecture Notes in Pure and Applied Mathematics, Vol. 196, Marcel Dekker, New York, 1998.

23. Q. Lin and N. Yan, Construction and analysis of high efficient finite elements (in Chinese), Hebei University Press, P.R. China, 1996.

24. R. Verfürth, A posteriori error estimation and adaptive mesh refinement techniques, Teubner Skripten zur Numerik, B.G. Teubner, Stuttgart, 1995.

25. L. B. Wahlbin, Superconvergence in galerkin finite element methods, Lecture Notes in Mathematics, Vol. 1605, Springer, Berlin, 1995.

26. J. Z. Zhu and Z. Zhang, The relationship of some a posteriori error estimators, Comput Methods Appl Mech Eng 176 (1999), 463–475.

27. D. Jerison, Ten lectures in free boundary problems, CBMS/NSF Reginal Conference, Wayne State University, Detroit, May 2003.